Simple denoising algorithm using wavelet transform

Manojit Roy, V. Ravi Kumar[1], B. D. Kulkarni
Chemical Engineering Division, National Chemical Laboratory, Pune 411 008, India
John Sanderson, Martin Rhodes
Department of Chemical Engineering, Monash University, Clayton, Victoria, 3168, Australia
Michel vander Stappen
Unilever Research, Vlaardingen, Postbox 114, 3130, AC Vlaardingen, The Netherlands

February 6, 2008

keywords: Noise, Discrete wavelet transform, Chaos, Differentiation

Application of wavelets and multiresolution analysis to reaction engineering systems from the point of view of process monitoring, fault detection, systems analysis etc. is an important topic and of current research interest (see, Bakshi and Stephanopoulos, 1994; Safavi et. al., 1997; Luo et. al., 1998; Carrier and Stephanopoulos, 1998). In the present paper we focus on one such important application, where we propose a new and simple algorithm for the reduction of noise from a scalar time series data. Presence of noise in a time–varying signal restricts one's ability to obtain meaningful information from the signal. Measurement of correlation dimension can get affected by a noise level as small as 1% of signal, making estimation of invariant properties of a dynamical

[1]e-mail address for correspondence: ravi@che.ncl.res.in

system, such as the dimension of the attractor and Lyapunov exponents, almost impossible (Kostelich and Yorke, 1988). Noise in experimental data can also cause misleading conclusions (Grassberger et. al., 1991). A host of literature exists on various techniques for noise reduction (Kostelich and Yorke, 1988; Härdle, 1990; Farmer and Sidorowich, 1991; Sauer, 1992; Cawley and Hsu, 1992; Cohen, 1995; Donoho and Johnstone, 1995; Kantz and Schreiber, 1997). For instance, Fast Fourier Transform (FFT) reduces noise effectively in those cases where the frequency distribution of noise is known (Kostelich and Yorke, 1988; Cohen, 1995; Kantz and Schreiber, 1997); singular value analysis methods (Cawley and Hsu, 1992) project the original time–series onto an optimal subspace, whereby noise components are left behind in the remaining orthogonal directions, etc. In the existing wavelet–based denoising methods (Donoho and Johnstone, 1995) two types of denoising are introduced: linear denoising and nonlinear denoising. In linear denoising, noise is assumed to be concentrated only on the fine scales and all the wavelet coefficients below these scales are cut off. Nonlinear denoising, on the other hand, treats noise reduction by either cutting off all coefficients below a certain threshold (so called 'hard–thresholding'), or reducing all coefficients by this threshold (so called 'soft–thresholding'). The threshold values are obtained by statistical calculations and has been seen to depend on the standard deviation of the noise (Nason, 1994).

The noise reduction algorithm that we propose here makes use of the wavelet transform (WT) which in many ways complements the well known Fourier Transform (FT) procedure. We apply our method, firstly, to three model flow systems, *viz.* Lorenz, Autocatalator, and Rössler systems, all exhibiting chaotic dynamics. The reasons for choosing these systems are the following: Firstly, all of them are simplified models of well–studied experimental systems. For instance, Lorenz is a simple realization of convective systems (Lorenz, 1963), while the Autocatalator and Rössler have their more complicated analogs in chemical multicomponent reactions (Rössler, 1976; Lynch, 1992). Secondly, chaotic dynamics is extremely nonlinear, highly sensitive, possesses only short–time correlations and is associated with a broad range

of frequencies (Guckenheimer and Holmes, 1983; Strogatz, 1994). Because of these properties it is well known that FT methods are not applicable in a straightforward way to chaotic dynamical systems (Abarbanel, 1993). On the other hand, WT methods are particularly suited to handle not only nonlinear but nonstationary signals (Strang and Nguyen, 1996). This is because the properties of the data are studied at varying scales with superior time localization analysis when compared to FT technique. Our noise reduction algorithm is advantageous, because, as shall be shown, the threshold level for noise is identified automatically. In this study, we have used the discrete analog of the wavelet transform (DWT) which involves transforming a given signal with orthogonal wavelet basis functions by dilating and translating in discrete steps (Daubechies, 1990; Holschneider, 1995). For study purposes we corrupt one variable $x(t)$ for each of these systems with noise of zero mean, and then apply our algorithm for denoising. We analyze the performance of this method in all the three systems for a wide range of noise strengths, and show its effectiveness. Importantly, we then validate the applicability of the method to experimental data obtained from two chemical systems. In one system the time series data was obtained from pressure fluctuation measurements of the hydrodynamics in a fluidized bed. In the other the conductivity measurements in a liquid surfactant manufacturing experiment were analyzed.

Methodology

The noise reduction algorithm based on DWT consists of the following five steps:

Step 1:

In first step, we differentiate the noisy signal $x(t)$ to obtain the data $x_d(t)$, using the method of central finite differences with fourth order correction to minimize error (Constantinides, 1987), *i.e.*,

$$x_d(t) \quad = \quad \frac{dx(t)}{dt} \, . \tag{1}$$

Step 2:

We then take DWT of the data $x_d(t)$ and obtain wavelet coefficients $W_{j,k}$ at various *dyadic scales* j and displacements k. A dyadic scale is the scale whose numerical magnitude is equal to 2 (two) raised to an integer exponent, and is labeled by the exponent. Thus, the dyadic scale j refers to a scale of magnitude 2^j. In other words, it indicates a resolution of 2^j data points. Thus a low value of j implies finer resolution while high j analyzes the signal at coarser resolution. This transform is the discrete analog of continuous WT (Holschneider, 1995), and is given by the formula

$$W_{j,k} \quad = \quad \int_{-\infty}^{+\infty} x_d(t)\ \psi_{j,k}(t)\ dt\ , \tag{2}$$

with

$$\psi_{j,k}(t) \quad = \quad 2^{j/2}\psi(2^j t - k)$$

where j, k are integers. As for the wavelet function $\psi(t)$ we have chosen Daubechies compactly supported orthogonal function with four filter coefficients (Daubechies, 1990; Press et. al., 1996).

Step 3:

In this step we estimate the *power* P_j contained in different dyadic scales j, via

$$P_j(x) \quad = \quad \sum_{k=-\infty}^{+\infty} |W_{j,k}|^2 \quad (j = 1, 2, \cdots) \tag{3}$$

By plotting the variation of P_j with j, we see that it is possible to identify a scale j_m at which the power due to noise falls off rapidly. This is important because as we shall see from the studies of the case examples that it provides a mean for automation in detection of threshold. The identification of the scale j_m at which power due to noise shows the first minimum allows us to reset all $W_{j,k}$ upto scale j_m to zero, *i.e.*, $W_{j,k} = 0$, for $j = 1, 2, \cdots, j_m$.

Step 4:

In the fourth step, we reconstruct the denoised data $\hat{x}_d(t)$ by taking inverse transform of the coefficients $W_{j,k}$:

$$\hat{x}_d(t) \quad = \quad c_\psi \sum_{j=0}^{\infty} \sum_{k=-\infty}^{\infty} W_{j,k}\, \psi_{j,k}(t)\ , \tag{4}$$

where c_ψ is normalization constant given by

$$c_\psi \quad = \quad 1/\int_{-\infty}^{\infty} \frac{|\hat{\psi}(\omega)|^2}{\omega} d\omega \ < \ \infty\ ,$$

with $\hat{\psi}(\omega)$ as the Fourier transform of the wavelet function $\psi(t)$.

Step 5:

In the fifth and final step $\hat{x}_d(t)$ is integrated to yield the cleansed signal $\hat{x}(t)$:

$$\hat{x}(t) \quad = \quad \int \hat{x}_d(t) dt\ . \tag{5}$$

There exists a commutativity property between the operation of differentiation/integration and wavelet transform. Therefore first differentiating the signal and then taking DWT is equivalent to carrying out the two operations in reverse order. This implies that the same result can be obtained by switching the order between the first and second steps, and then between the fourth and fifth.

The effectiveness of the method lies in the following observations. Upon differentiation, contribution due to white noise moves towards the finer scales because the process of differentiation converts the uncorrelated stochastic process to a first order moving average process and thereby distributes more energy to the finer scales. That the differentiation of white noise brings about this behavior is known in the Fourier spectrum (Box et. al., 1994). It may be noted that the nature and effectiveness of separation depend on the wavelet basis function chosen and also on the properties of the derivatives of WT, which is in itself a highly interesting and not fully understood subject (Strang and

Nguyen, 1996). For the signals studied in this paper, model as well as experimental, the wanted signal features lie in the coarser wavelet scales while the unwanted signal features after differentiation lie in the finer resolution wavelet scales. This is because the size of the data set handled decides the total number of scales available and a suitable choice can bring out the noisy signal WT features lying in the coarser scales. This justifies the assumption that fine scale features can be removed by setting the corresponding wavelet coefficients to zero and coarse scale features retained after differentiation. For this reason we also see a clear separation in the scales attributed to noise and those for the signal. A threshold scale for noise removal is thus identified and this leads to an automation for noise removal.

Result and Discussion

We first take up the three model systems and discuss the observations. For test purposes the pure signal obtained from these systems were corrupted with noise of certain strength. For the systems chosen for study, *viz.*, Lorenz, Autocatalator, and Rössler, Table 1 summarizes the details, *i.e.* the equations governing their dynamics, the values chosen for the parameters, and the nature of the evolution of these systems for these sets of parameter values. These values were chosen appropriately so that the dynamics is chaotic. In our initial studies, purely for testing purposes, we studied situations where we ensure that all scales are affected by noise. In the wavelet domain this can be conveniently carried out by perturbing the wavelet coefficients in the following way. The differential equations are first numerically integrated to obtain pure signal $x^0(t_i)$ at equidistant time steps t_i. We then take DWT of the signal, and add white noise η of zero mean and certain strength, *i.e.*, $W_{j,k} = W^0_{j,k} + \eta$, where $W^0_{j,k}, W_{j,k}$ are the wavelet coefficients of pure and noisy signals respectively. We take the strength of noise as the relative percentage of the difference between the maximum and minimum of the signal value. Since each coefficient $W_{j,k}$ is individually affected by the noise, this procedure ensures equal weightage for presence of noise at all scales. Reconstructing the time series signal with this perturbed set of wavelet coefficients gave us the noisy signal to be

cleansed. Our studies in this fashion did show that noise and signal separation was achieved. For the subsequent studies we followed the usual way of corrupting the signal by additive noise, *i.e.*,

$$x(t_i) = x^0(t_i) + \eta(t_i) \ , \tag{6}$$

where $\eta(t_i) \in [-.5, .5]$ is the noise with zero mean and uniform distribution, and J the number of available dyadic scales. We have taken data size of 16384 $(= 2^{14})$ points for all these three systems, and so $J = 14$.

In Fig. 1 we plot our observations for the Lorenz system. Fig. 1 (a) shows the power at different scales in the pure signal $x^0(t_i)$. In Fig. 1 (b) we plot the scalewise power distribution after numerically differentiating the pure signal. We see that almost the entire power of the differentiated data is accumulated within the dyadic scales 4 and 9 (the signal power between scales 10 and 14 has disappeared by the process of differentiation). Fig. 1 (c) plots the scalewise power in the noisy signal $x(t_i)$ when the pure signal is infected with noise $\eta(t_i)$ of a typical strength of 5% of the signal (that is, 5% of the difference in the maximum and minimum values of $x^0(t_i)$). Because of the relative larger contribution at all scales from the pure signal, compared to that from noise, it is impossible to distinguish between the two components, and the figure looks qualitatively very similar to Fig. 1 (a). However, when we plot the scalewise power distribution of the differentiated noisy data in Fig. 1 (d), the signal contribution can easily be identified and also compared with the plot in Fig. 1 (b). It is to be noted that the difference in the values of the two peaks in Figs. 1 (b) and (d) arises because of the power being normalized by the respective total signal power. The contribution due to noise shows up in the finer scales. A clear minimum with close to zero value separates out two distinct regions. Fig. 1 (e) exhibits a small segment of the signal after the noise has been successfully removed following the procedure outlined above. All the three signals – pure, noisy, and cleansed – are overlaid for the sake of comparison.

In Fig. 2 we show the results for the Autocatalator and the Rössler reacting

systems. Fig. 2 (a) and (c) plot, respectively, the scalewise power distribution for noise–infected signals obtained from the two systems. Like in the case of Lorenz system, it is evident that here also one cannot distinguish the noise and signal components. Fig. 2 (b) and (d) exhibit scalewise power profile for the differentiated data of the two signals respectively. The clear separation is again obvious.

In order to quantitatively estimate the efficiency of our denoising method, we have made the following error estimation (Kostelich and Schreiber, 1993) for the above three model systems. Since in all these cases the pure signal is known, a measure of the amount of error present in the cleaned data is obtained by taking rms deviation of the cleaned signal $\hat{x}(t_i)$ from the pure signal $x^0(t_i)$ as follows,

$$\hat{E} = \Big(\frac{1}{N}\sum_{i=1}^{N}(\hat{x}(t_i) - x^0(t_i))^2\Big)^{1/2}, \tag{7}$$

where N is the length of the time series. Similar quantity E for the noisy data $x(t_i)$ is also computed. The condition $\hat{E}/E < 1$ guarantees that noise has been successfully reduced. The error estimator $\hat{E}/E$ is a natural measure for noise reduction when the original dynamics is known (Kostelich and Schreiber, 1993). In Fig. 3 we plot $\hat{E}/E$ against noise strength, for the three model systems. We see that for the entire range of noise values, and even with noise level as high as 10% of the signal exhibiting chaotic dynamics, $\hat{E}/E$ remains appreciably below unity. Thus the plot demonstrates the efficiency of the approach. Different wavelet basis functions may change the nature and also improve the efficiency further.

We now discuss our method when applied to raw data obtained from two real chemical systems. In the first system, the time series data was obtained from the measurements of the pressure fluctuations in a fluidized bed, which consists of a vertical chamber inside of which a bed of solid particles is supported by an upwardly moving gas. Our system used a bed of silica sand particles (of mean diameter 200 microns) with a settled height of 500 mm, fluidized by ambient air in a transparent vessel 430 mm across and 15 mm

wide. Beyond a critical inlet gas velocity, *viz.* the minimum bubbling velocity, the gas passes through the bed in the form of bubbles, thereby churning the solid and gas mixture in a turbulent manner. The time series data have been taken by measuring the pressure fluctuations inside this mixture, relative to atmospheric pressure, using a pressure transducer attached to a probe inserted into the fluid bed. The bed was operated at an inlet gas velocity of 0.85 m/sec, and the pressure fluctuations were recorded at a sampling rate of 333 Hz (333 data points per second). As a standard procedure, we normalize the data by subtracting mean and dividing by standard deviation (Constantinides, 1987; Bai et. al., 1997). In Fig. 4 we show the results obtained after the data have been subjected to denoising. Fig. 4 (a) shows the power distribution at different scales in the original experimental signal, while in Fig. 4 (b) we plot the scalewise power profile of the differentiated data. Again one clearly sees the two distinct contributions due to the noise and signal components. Fig. 4 (c) shows short segments of the denoised signal and the original signal which is overlaid for comparison. The cleaned signal is seen to be smooth indicating that the noise has been removed.

In the second chemical system, the time series data was obtained by sampling a measure related to the conductivity in a 3 liter liquid surfactant manufacturing experiment, at a sampling rate of 500 Hz. The time series is highly nonstationary since at various stages the operational parameters are altered (increasing the temperature for certain duration, then adding actives to the liquid, etc.). We studied unfiltered noisy data sets from the experiments, in order to check if our method can filter the noise out and also bring forth some intrinsic features of the system. We used our denoising algorithm to treat this data set in a slightly different way. The aim was to remove the finer scales from the differentiated data one by one, starting from the lowest (dyadic scale 1) and gradually going up, so that at each stage (after integrating the data) the observable frequencies in the filtered signal may be related to identifiable physical sources. Fig. 5 (a) shows a small segment (1 second long) of the noisy data. In Fig. 5 (b) we plot, on the same scale as in the earlier figure, the filtered data, using our method to remove the lowest dyadic scale 1. One

can now clearly identify a 50 Hz component, due to the signal from electrical power supply (the 'net frequency'). By removing scale 2 alongwith scale 1, the net frequency goes away, and the filtered data exhibits a 13 Hz component superimposed with occasional spikes. This 13 Hz signal shows up clearly in the filtered data with scale 3 also removed. The same Fig. 5 (b) shows this data, overlaid on the data with scale 1 removed. This 13 Hz may have arisen from the stirring device which has two blades and revolves with 260 rpm, corresponding to approximately 10 Hz. The electronic signal had an antialiasing feature of no more than 250 Hz and therefore aliasing (beating) may be ruled out. It may also be mentioned here that the Fourier power spectrum of the denoised signal shows a spike at 50 Hz frequency, whose removal resulted in a residual spectrum consisting mainly of a background continuum without any appreciable peak around 13 Hz. This study with the present example suggests that the wavelet transform methodology offers considerable benefits in the recovery of intrinsic signal components.

Summary

We have presented a new and alternative algorithm for noise reduction using discrete wavelet transform. We believe that our algorithm will be beneficial in various noise reduction applications, and that it shows promise in developing techniques which can resolve an observed signal into its various intrinsic components. In our method the threshold for reducing noise comes out automatically. The algorithm has been applied to three model flow systems - Lorenz, Autocatalator, and Rössler systems - all evolving chaotically. The method is seen to work quite well for a wide range of noise strengths, even as large as 10% of the signal level. We have also applied the method successfully to noisy time series data obtained from the measurement of pressure fluctuations in a fluidized bed, and also to that obtained by conductivity measurement in a liquid surfactant experiment. In all the illustrations we have been able to observe that there is a clean separation in the frequencies covered by the differentiated signal and white noise. However, if the noise is colored, a certain degree of overlap between the signal and noise may exist even after

differentiation. For this complex situation, the method needs to be improved upon.

Acknowledgement

Authors acknowledge Unilever Research, Port Sunlight, for financial and other assistance. Part of the work has been carried out under the aegis of Indo–Australian S&T program DST/INT/AUS/I–94/97.

Literature cited

Abarbanel, H. D. I., "The Observance of Chaotic Data in Physical Syatems", Rev. Mod. Phys. 65, 1340 (1993)

Bai, D., T. Bi, and J. R. Grace "Chaotic Behavior of Fluidized Beds Based on Pressure and Voidage Fluctuations", AIChE Journal 43, 1357 (1997)

Bakshi, B., and G. Stephanopoulos "Representation of Process Trends. Part IV. Induction of Real–time Patterns from Operating Data for Diagnoses and Supervisory Control", Computers chem. Engng. 18, 303 (1994)

Box, G. E. P., G. M. Jenkins and G. C. Reinsel, "Time Series Analysis Forecasting and Control" Prentice Hall, Englewood Cliffs (1994)

Carrier, J. F., and G. Stephanopoulos "Wavelet–Based Modulation in Control–Relevant Process Identification", AIChE Journal 44, 341 (1998)

Cawley, R., and G.–H. Hsu "Local–Geometric–Projection Method for Noise Reduction in Chaotic Maps and Flows", Phys. Rev. A 46, 3057 (1992)

Cohen, L., "Time frequency analysis" Prentice Hall, Englewood Cliffs (1995)

Constantinides, A., "Applied Numerical Methods with Personal Computers"

McGraw–Hill Book Company, USA (1987)

Daubechies, I., "Ten Lectures on Wavelets" SIAM, Philadelphia (1990)

Donoho, D. L., and I. M. Johnstone "Adapting to Unknown Smoothness via Wavelet Shrinkage", J. American Statistical Association 90, 1200 (1995)

Farmer, J. D., and J. J. Sidorowich "Optimal Shadowing and Noise Reduction", Physica D 47, 373 (1991)

Grassberger, P., T. Schreiber, and C. Schaffrath "Non–linear Time Sequence Analysis", Int. J. Bifurcation Chaos 1, 521 (1991)

Guckenheimer, E. and P. Holmes, "Nonlinear Oscillation, Dynamical Systems and Bifurcations of Vector Fields" Springer Verlag, Berlin (1983)

Härdle, W., "Applied Nonparametric Regression" Econometric Society Monographs, Cambridge University Press (1990)

Holschneider, M., "Wavelets: An Analysis Tool" Clarendon Press, Oxford (1995)

Kantz, H. and T. Schreiber, "Nonlinear Time Series Analysis" Cambridge University Press, Cambridge (1997)

Kostelich, E. J., and J. A. Yorke "Noise Reduction in Dynamical Systems", Phys. Rev. A 38, 1649 (1988)

Lorenz, E. "Deterministic Nonperiodic Flow", J. Atmos. Sc. 20, 130 (1963)

Luo, R., M. Misra, S. J. Qin, R. Barton, and D. M. Himmelblau "Sensor Fault Detection via Multiscale Analysis and Nonparametric Statistical Inference", Ind. Eng. Chem. Res. 37, 1024 (1998)

Lynch, D. T. "Chaotic Behavior of Reaction Systems: Mixed Cubic and Quadratic Autocatalators", Chem. Engg. Sci. 47, 4435 (1992)

Nason, G. P., "Wavelet Regression by Cross–validation" Dept. of Mathematics, University of Bristol (1994)

Press, W. H., B. P. Flannery, S. A. Teukolsky and W. T. Vetterling, "Numerical Recipes" Cambridge University Press, Cambridge (1987)

Rössler, O. E. "Chaotic Behavior in Simple Reaction Syatems", Z. Naturforsch. 31 a, 259 (1976)

Safavi, A. A., J. Chen, and J. A. Romagnoli "Wavelet–Based Density Estimation and Application to Process Monitoring", AIChE Journal 43, 1227 (1997)

Sauer, T. "A Noise Reduction Method for Signals from Nonlinear Systems", Physica D 58, 193 (1992)

Strang, G. and T. Nguyen, "Wavelets and Filter Banks" Wellesley–Cambridge Press (1996)

Strogatz, S. H., "Nonlinear Dynamics and Chaos: With Applications to Physics, Biology, Chemistry and Engineering" Addison–Wesley (1994)

Figure Captions

Fig. 1. Plots for Lorenz system, with parameter values as stated in Table 1. 16384 ($= 2^{14}$) data points are considered. Scalewise power distribution is plotted against the dyadic scale, (a) for the pure signal (the interpolated line through the data points is drawn for visualization), (b) using the data obtained after differentiating the signal, (c) for the signal corrupted by noise, and (d) using differentiated data of noisy signal. A segment of cleansed signal is shown in (e), alongwith the pure and noisy signals overlaid for comparison.

Fig. 2. Plots for Autocatalator and Rössler systems, in (a), (b) and (c), (d) respectively, for parameter values as in Table 1. Scalewise power profile plotted, (a) for the noisy autocatalytic signal, (b) using data after differentiating the signal, (c) for noisy Rössler signal, and (d) using the differentiated data of noisy signal.

Fig. 3. The error estimator $\hat{E}/E$ plotted against the noise strength for all the three systems.

Fig. 4. Plots for the fluidized bed experiment. (a) Scalewise power profile is shown, for (a) the experimental signal, and (b) the data after the signal has been numerically differentiated. A small segment of the cleansed signal is shown in (c), alongwith the original signal for comparison.

Fig. 5. Plots for the liquid surfactant experiment. (a) A segment of the original noisy data, 1 second long. (b) The filtered data, with scale 1 removed, and with scales 1, 2 and 3 removed (on the same axes–scales as (a)).

Table 1: Various model systems studied, alongwith their parameter values and nature of dynamics.

Systems	Lorenz	Autocatalator	Rössler
Dynamical equations	$dx/dt = -\sigma x + \sigma y,$ $dy/dt = Rx - y - xz,$ $dz/dt = -bz + xy.$	$dx/dt = 1 - x - Da_1 xz^2,$ $dy/dt = \beta - y - Da_2 yz^2,$ $dz/dt = 1 - (1 + Da_3)z$ $+\alpha(Da_1 x + Da_2 y)z^2.$	$dx/dt = -y - z,$ $dy/dt = x + ay,$ $dz/dt = b$ $+z(x - c).$
Parameters chosen	$\sigma = 10,\ R = 28,$ $b = 8/3.$	$Da_1 = 18000,\ Da_2 = 400,$ $Da_3 = 80,\ \beta = 2.93,$ $\alpha = 1.5.$	$a = .398,\ b = 2,$ $c = 4.$
Dynamics	Chaotic	Chaotic	Chaotic

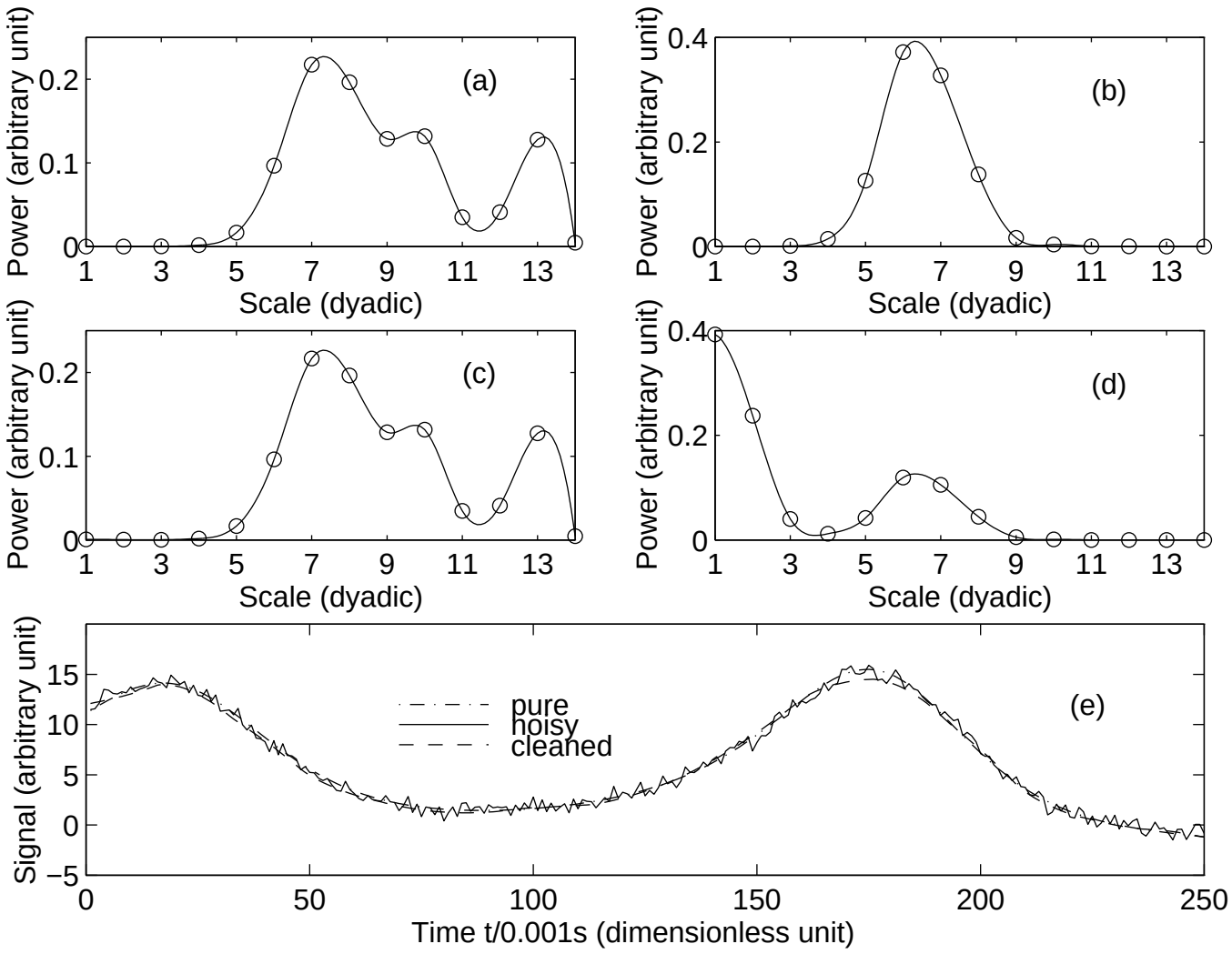
Power (arbitrary unit)
Scale (dyadic)
(a)
(b)
(c)
(d)
Signal (arbitrary unit)
Time t/0.001s (dimensionless unit)
pure
noisy
cleaned
(e)

FIG. 1 (Roy)

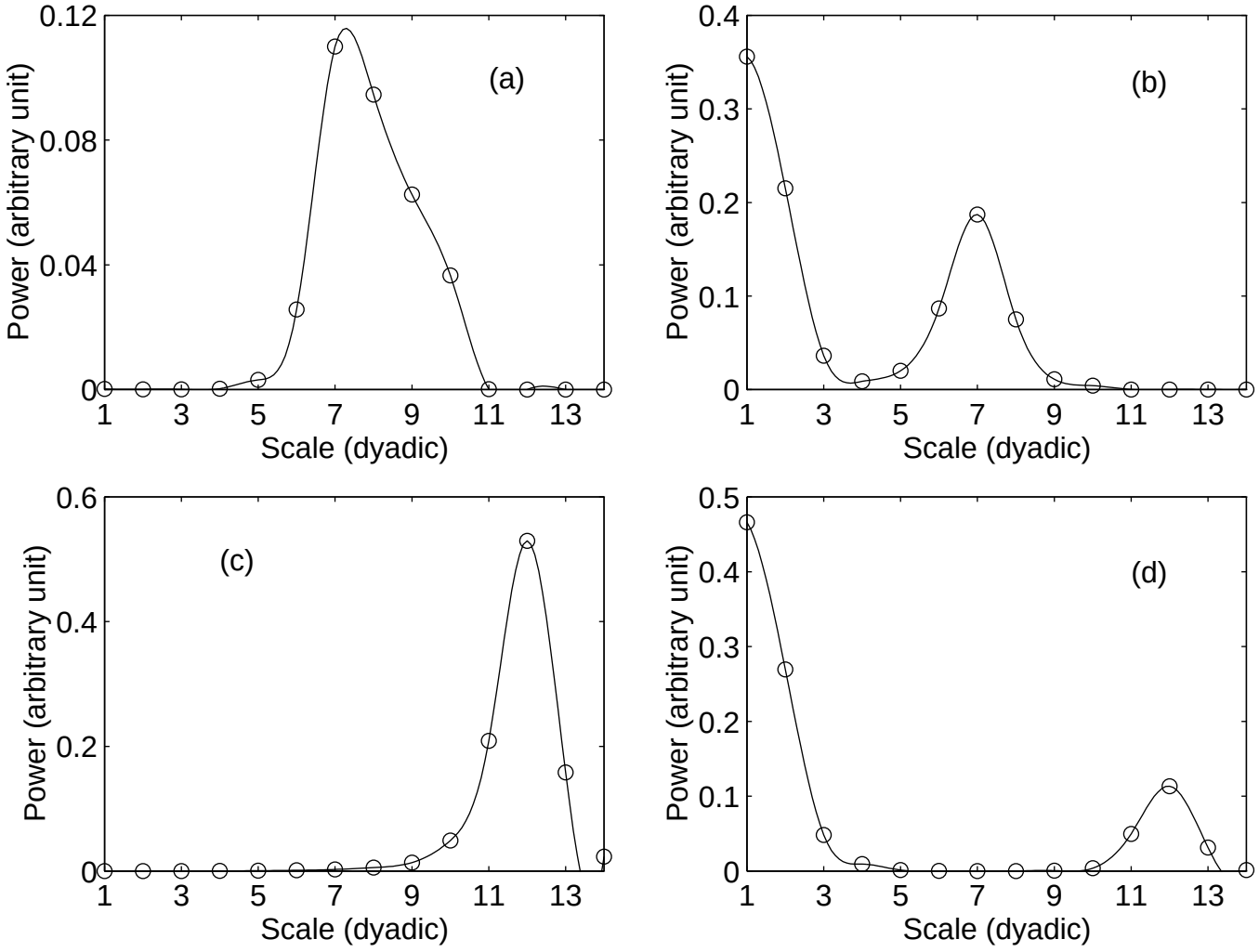
(a)
(b)
(c)
(d)
Power (arbitrary unit)
Scale (dyadic)
0.12
0.08
0.04
0
0.4
0.3
0.2
0.1
0.6
0.5
1
3
5
7
9
11
13

FIG. 2 (Roy)

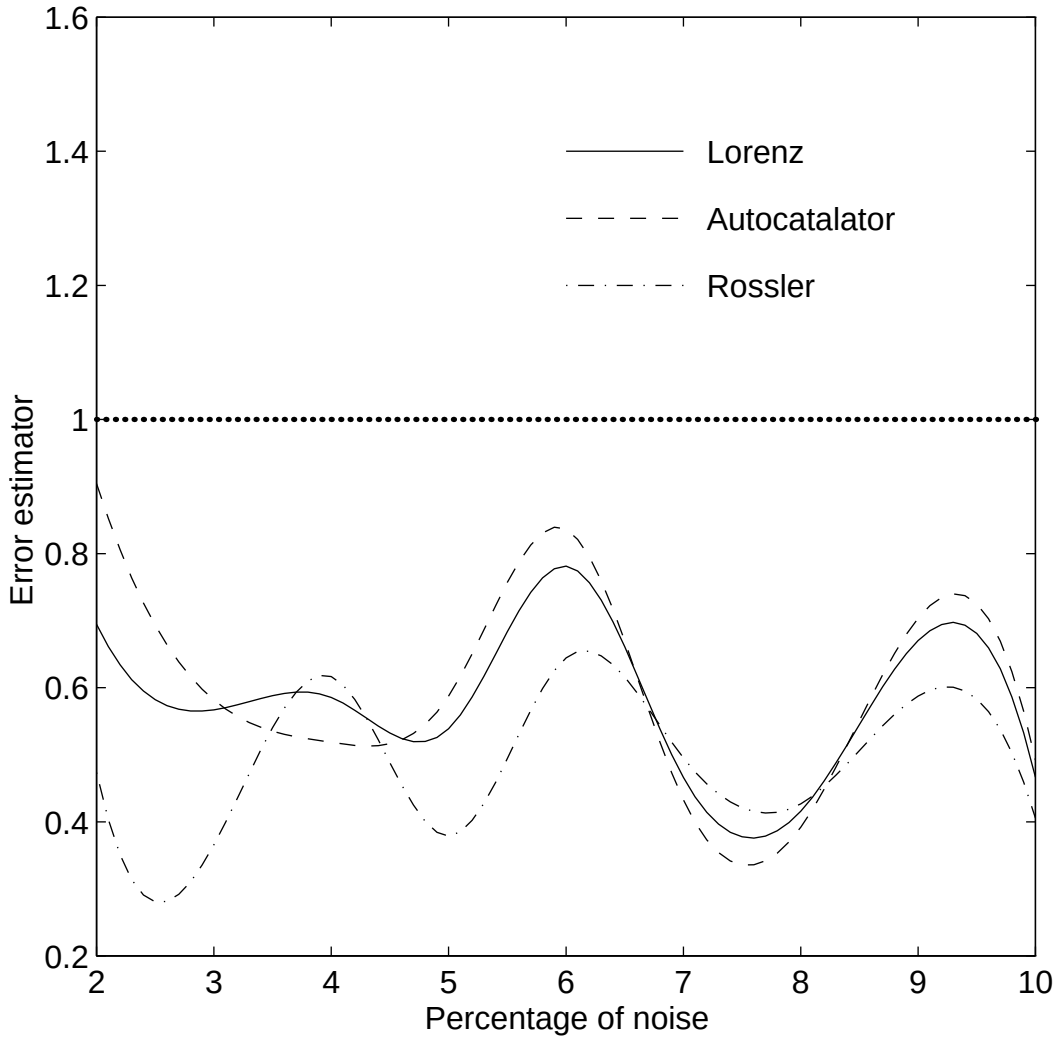
1.6
1.4
1.2
1
0.8
0.6
0.4
0.2
Error estimator
2
3
4
5
6
7
8
9
10
Percentage of noise
Lorenz
Autocatalator
Rossler

FIG. 3 (Roy)

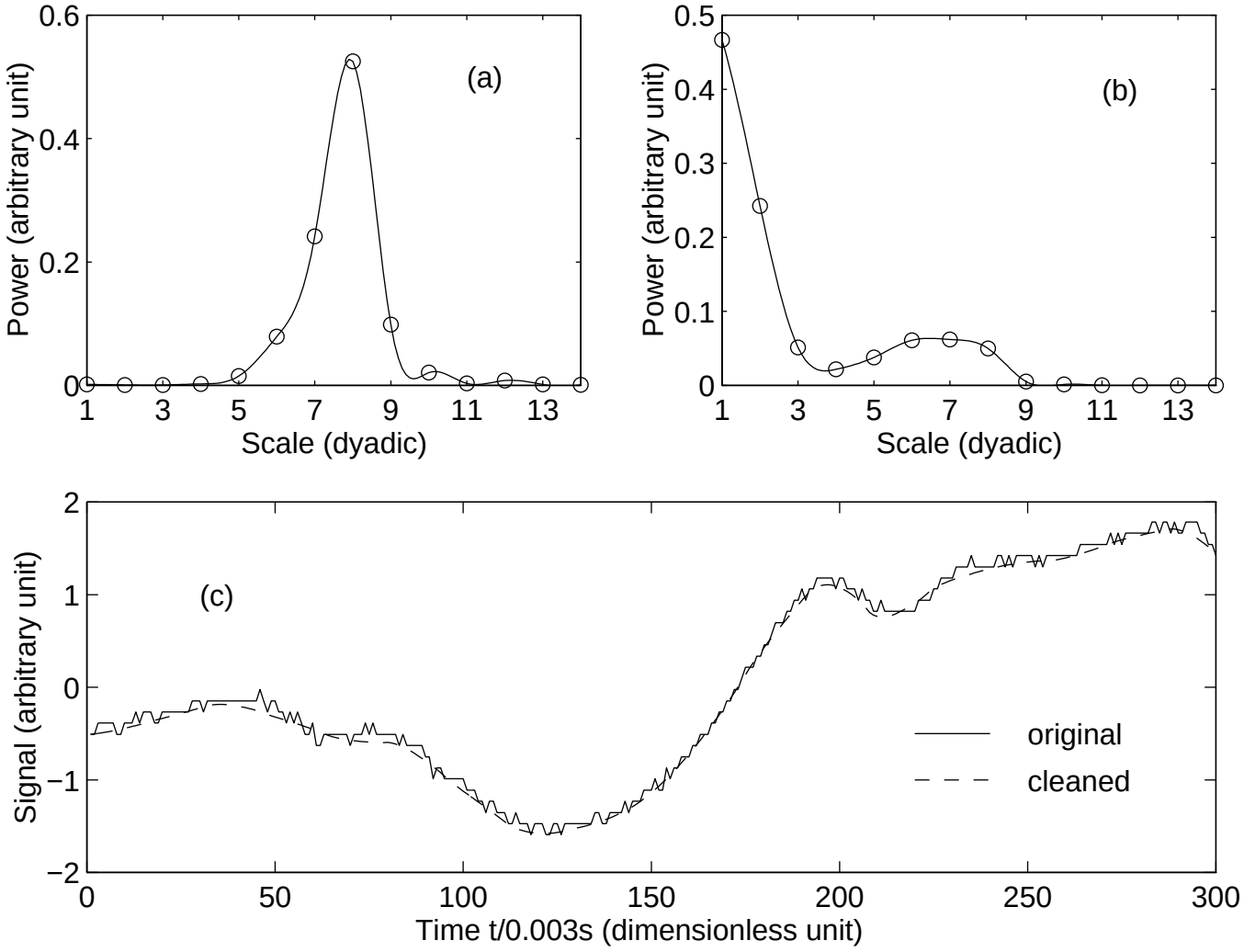
(a)
Power (arbitrary unit)
Scale (dyadic)
(b)
Power (arbitrary unit)
Scale (dyadic)
(c)
Signal (arbitrary unit)
original
cleaned
Time t/0.003s (dimensionless unit)

FIG. 4 (Roy)

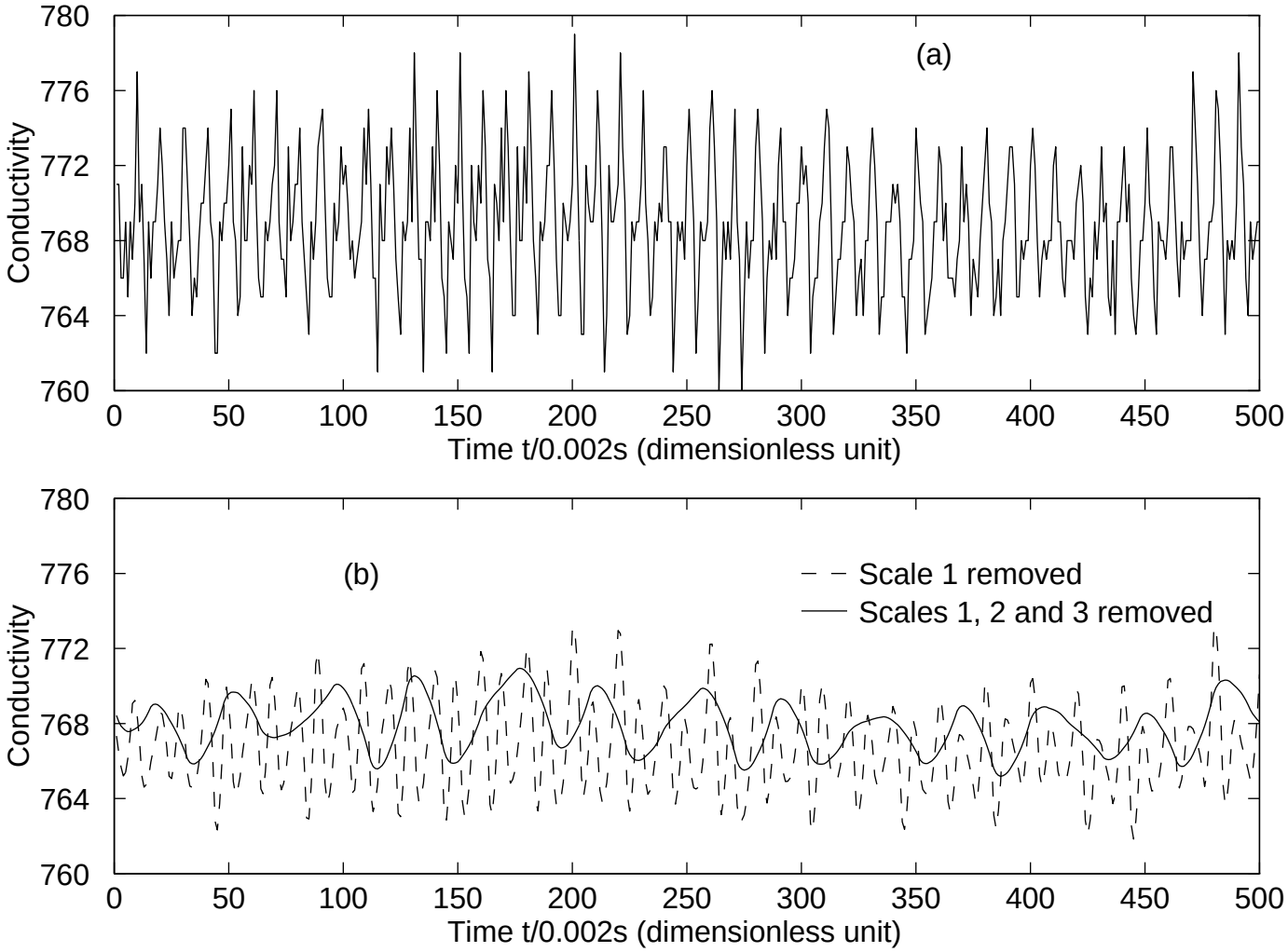
780
776
772
768
764
760
Conductivity
(a)
0
50
100
150
200
250
300
350
400
450
500
Time t/0.002s (dimensionless unit)
780
776
772
768
764
760
Conductivity
(b)
Scale 1 removed
Scales 1, 2 and 3 removed
0
50
100
150
200
250
300
350
400
450
500
Time t/0.002s (dimensionless unit)

FIG. 5 (Roy)